Published in final edited form as:
Transgenic Res. 2012 April ; 21(2): 393–406. doi:10.1007/s11248-011-9529-3.

Molecular characterizations of *Nop16* in murine mammary tumors with varying levels of c-*Myc*

Donald W. Kundel,
Department of Pathology, University of Minnesota Medical School-Duluth Campus, 1035 University Drive, Duluth, MN 55812, USA

Emily Stromquist,
Department of Physiology and Pharmacology, University of Minnesota Medical School-Duluth Campus, 1035 University Drive, Duluth, MN 55812, USA

Amy L. Greene,
Department of Biomedical Sciences, Mercer University School of Medicine, Savannah, GA 31404, USA

Olga Zhdankin,
Department of Physiology and Pharmacology, University of Minnesota Medical School-Duluth Campus, 1035 University Drive, Duluth, MN 55812, USA

Ronald R. Regal, and
Department of Mathematics and Statistics, University of Minnesota Duluth, 1035 University Drive, Duluth, MN 55812, USA

Teresa A. Rose-Hellekant
Department of Physiology and Pharmacology, University of Minnesota Medical School-Duluth Campus, 1035 University Drive, Duluth, MN 55812, USA

Teresa A. Rose-Hellekant: trosehel@d.umn.edu

Abstract

NOP16, also known as *HSPC111*, has been identified as a MYC and estrogen regulated gene in in vitro studies, hence coexpression levels were strongly correlated. Importantly, high expression of *NOP16* was associated with poor clinical outcome in breast cancer patients. However, coexpression of *NOP16*, *MYC* and estrogen receptor (*ESR1*) varied widely in tumors and cell lines suggesting that transcriptional regulation differed according to pathological environments. The goal of this study was to determine the expression patterns of *Nop16*, *Myc* and *Esr1* in murine mammary tumors with disparate histopathological and molecular features. We hypothesized that tumor environments with relatively high *Myc* levels would have different coexpression patterns than tumor environments with relatively low *Myc* levels. We measured levels of *Myc* and *Nop16* mRNA and protein in tumors from WAP-c-myc mice that were of high grade and metastasized

Correspondence to: Teresa A. Rose-Hellekant, trosehel@d.umn.edu.

Electronic supplementary material The online version of this article (doi:10.1007/s11248-011-9529-3) contains supplementary material, which is available to authorized users.

frequently. In contrast, *Myc* and *Nop16* mRNA and proteins levels were significantly lower in the less aggressive tumors that developed in NRL-TGFα mice. Tumors from both mouse lines express ESR1 protein and we found that *Esr1* mRNA levels correlated positively with *Myc* levels in both models. However, *Myc* and *Nop16* transcript levels correlated positively only in tumors from NRL-TGFα mice. We identified prominent NOP16 protein in nuclei and less prominent staining in the cytoplasm of luminal cells of ducts and lobules from normal mammary glands as well as in hyperplasias and tumors obtained from NRL-TGFα mice. This staining pattern was reversed in tumors from WAP-c-Myc mice as nuclear staining was faint or absent and cytoplasmic staining more pronounced. In summary, the regulation of expression and localization of NOP16 varies in tumor environments with high versus low MYC levels and demonstrate the importance of stratifying clinical breast cancers based on MYC levels.

Keywords

NOP16; MYC; Breast cancer biomarkers; Transgenic mouse models

Introduction

The ability to make valid risk assessments, treatment decisions and outcome predictions for human breast cancers is dependent upon detailed understanding of the disease processes and identification of therapeutic targets. Current tools for obtaining such information include studies from biopsy samples of human breast tumors and from breast cancer cell lines. In addition, animal models that share characteristics of human breast cancer provide valuable platforms for obtaining in vivo information about cancer risk, tumor development and efficacy of targeted therapeutics.

There is a growing list of novel putative breast cancer biomarkers identified as genomic profiles of chromosomal aberrations, gene sets identified through tumor global gene expression analysis (Perou et al. 2000) or their immunohistochemical proxy, as well as single biomarkers which correlate to patient outcome and treatment success (Geyer et al. 2009, Ma et al. 2009). Immunotyping for the presence of estrogen receptor alpha (ESR1), progesterone receptors (PGR) and HER2 have identified patients likely to benefit from biomarker specific therapies. However, in spite of these stratifications and the application of targeted therapies, there are yet wide variations in treatment outcome and survival partly because some tumors lack stratifying biomarkers and partly because some tumors with stratifying biomarkers fail to respond to the targeted therapy. These results indicate a critical need to deepen our understanding of breast cancer biology and the mechanisms that render tumor cells treatment-resistant.

One recently identified putative breast cancer biomarker is the *NOP16* gene, also referred to as *HSPC111* and *EMU4*. High mRNA expression of this gene has been correlated with poor breast cancer survival in human patients and with an aggressive phenotype in breast cancer cell lines (Butt et al. 2008) The function of NOP16 protein is largely unknown, although it belongs to a family of genes with ribosomal functions (Leung et al. 2006; Dai and Lu 2008; Ahmad et al. 2009) and has been localized to the large RNA-dependent nucleolar complex

in MCF7 breast cancer cells (Butt et al. 2008). In addition, *NOP16* mRNA was originally identified in a screen of genes upregulated by MYC and estrogen (Lin et al. 2004; McNeil et al. 2006; Dai and Lu 2008). Furthermore, in multiple breast cancer cell lines, *NOP16* mRNA levels were increased by induced MYC expression and addition of estrogen. However, in human breast cancers *NOP16* mRNA levels had a weak positive correlation to *MYC* mRNA and levels ranged similarly in tumors which were ESR1+ and ESR1− (Butt et al. 2008). These discordant data in human cell lines versus tumors support the need to further probe the transcriptional activities of NOP16 in carcinogenesis.

In the present study, we carried out molecular characterizations of *Nop16* mRNA and protein expression in the WAP-c-Myc and NRL-TGFα transgenic mouse models of estrogen receptor positive mammary cancers in which tumors expressed high versus low levels of the MYC oncogene. We demonstrate differences in *Nop*16 expression patterns in the dissimilar tumor environments from these two mouse lines. Taken together these data further support the need to stratify ESR1+ breast cancers and point to NOP16 and MYC as stratifying candidates.

Methods

Mice

WAP-c-Myc line 3507-1, designated TgN(WAP-Myc)212Bri, and NRL-TGFα line 1372-1 transgenic mice, designated TgN(NRL-tgfa)29EPS have been described (Sandgren et al. 1995; Rose-Hellekant and Sandgren 2000). The WAP (whey acidic protein) and NRL (neurelated lipocalin; more recently designated as lipocalin 2) promoters direct transgene expression to the luminal epithelial compartment. Transgenic mice were evaluated as heterozygotes. FVB/N breeder mice were acquired from Taconic and offspring of in-house bred animals were evaluated in this study as controls. Mice were housed in AAALAC accredited facilities in accordance with the Guide for the Care and Use of Laboratory Animals. Food (Lab Diet 5015) and water were provided ad libitum. All studies were approved by the Institutional Animal Care and Use Committee.

Western blot analysis of tumor containing mammary glands

Thirty mg of tissue were homogenized using a Polytron in 0.6 ml of T-PER Tissue Protein Extraction Reagent (Thermoscientific, cat. # 78510) containing 1.5 µl of Protease Inhibitors Cocktail (Sigma cat. # P8340). Samples were centrifuged at 10,000×*g* for 5 min to pellet tissue debris and supernatants were used for Western Blotting. Protein concentration in tissue lysates was detected using the Coomassie Plus Assay Kit (Thermoscientific, cat # 23236) and adjusted to 80 µg/µl, then samples were mixed with 2 X Laemmli Sample Buffer containing 5% beta mercaptoethanol, heated 5 min 95°C, and 40 µg of protein samples loaded (50 µl) on 8–16% Precast Gels (BIO-RAD, cat. # 161–1225). After separation, proteins were transferred to a nitrocellulose membrane. Membranes were blocked in Blotto (10% powdered milk in TBS-T buffer) and subjected to sequential antibody incubation. Primary antibodies and incubation conditions used include: Actin mouse monoclonal (Millipore cat. # P68133) 1:5,000 dilution in Blotto, incubated for 2 h at RT; NOP16 mouse polyclonal (AbCam cat # ab88449) 1:500 dilution in Blotto, incubated overnight at 4°C;

NOP16 rabbit polyclonal (Abnova, cat# H00051491-D01) 1:1000 dilution in Blotto, incubated overnight at 4°C. Secondary antibodies and conditions used include: ImmunoPure Goat Anti-Rabbit IgG Peroxidase Conjugated (Thermoscientific, cat # 31460) and ImmunoPure Goat Anti-Mouse IgG Peroxidase Conjugated (Thermoscientific, cat # 31430) 1:20,000 dilution in TBS-T, incubated for 1 h at r.t. Blots were treated with SuperSignal West Pico Chemiluminescent Substrate (Thermoscientific, cat # 34080) and images of blots captured on a FluorChem HD2 System. Spot density measurements were performed with auto background correction for NOP16 and Actin bands.

Quantitative gene expression analysis of mammary glands

Tissues were flash frozen in liquid nitrogen and stored at −70°C. RNA was isolated from tissues using RNAeasy kit (Qiagen). Expression levels of *Esr1*, *Pgr*, *Myc*, *Nop16* and the housekeeping gene *Pum1* were determined using methods described previously. Primers for *Esr1*, *Pgr*, and *Pum1* have been published (Rose-Hellekant et al. 2007). Primers used to detect *Nop16* were forward AAAGCGTCTGAACCGGAATGCT and reverse ACCTCCATGGCCTTTACCTTCT. Primers used to detect total *Myc* (endogenous and transgene) were forward AGTGCTGCATGAGGAGACAC and reverse GGTTTGCCTCTTCTCCACAG. Total RNA was isolated from frozen tissues, and 0.5–1.0 microgram of RNA were reverse transcribed to DNA in 20 microliters reaction volume using oligo(dTs) with the Affinity-Script QPCR cDNA Synthesis kit (Stratagene). Two control reactions were included; one was without Reverse Transcriptase and the other without RNA. PCR was performed using 2x Brilliant SYBR Green QPCR Master Mix (Stratagene). Triplicate cDNA samples were run and average crossing threshold (Ct) values calculated. Relative gene expressions were calculated as $2^{Ct(PUM1) - Ct(gene)}$. PUM1 was used as a normalizing gene.

Histology and immunohistochemistry

Tissues were fixed in 10% neutral buffered formalin at room temperature for 18–24 h, dehydrated in ethanol, embedded in paraffin, sectioned (4–6 μm), and stained with hematoxylin and eosin (H&E). Measurements of cytologic features and degree of hyperplasias were made with a microscope ocular grid calibrated with a hemocytometer. Immunohistochemical evaluations of estrogen receptor (ESR1; antibody #sc-542 Santa Cruz Biotechnology, Santa Cruz, CA, USA) and progesterone receptor (PGR; antibody #A0098, DakoCytomation, Carpinteria, CA, USA) were conducted as previously described (Rose-Hellekant et al. 2007) or as follows: deparaffinized slides were subjected to peroxidase blocking reagent (DakoCytomation, Carpinteria, CA, USA) followed by antigen retrieval using Rodent DECLOAKER for ESR1 and PGR (Biocare Medical, Concord, CA, USA) in a Pascal pressure cooker at 125°C for 20 min and 95°C for 35 min, rinsed with distilled water, then TBS (DakoCytomation) and protein blocked (DakoCytomation). Antigen retrieval for NOP16 immunohistochemistry (Abcam mouse polyclonal antibody raised against full length human protein) was in Tris-EDTA-Tween (TET) at 95°C for 35 min. Slides were then rinsed with TET and protein blocked for 10 min with Rodent M Blocker (Biocare Medical). Primary antibodies were added at 1:250 (ER) and 1:100 (PR) for 40 min and 1:15 (NOP16) overnight, then treated with Mouse on Mouse HRP Polymer (Biocare Medical) for 25 min, DAB for 5 min, DAB Enhancer S196 (DakoCytomation for ESR1 and PGR) and

counterstained with hematoxylin for 1–5 min prior to rinsing in water, dehydration through alcohols and a final rinse with Clear-Rite3 prior to coverslip mounting.

Nomenclature

Nomenclature generally followed recommendations by the Annapolis Group (Cardiff et al. 2000). It is accepted that human and mouse mammary tumors arise in terminal ducts or alveoli rather than in the larger collecting ducts, i.e. they arise in terminal ductal lobular units (TDLU). Growth of terminal ducts occurs at the slightly dilated terminal end buds. This developmental phase was defined as the ductal stage (D). Under hormonal influence there is budding from lateral and terminal portions of ducts producing the alveolar bud stage (AB). TDLU becomes complex and a cross section with up to 10 alveoli was classified as: lobular stage 1 (L1), between 11–35 alveoli as L2 and 36–100 alveoli as L3. When mammary glands displayed two lobular patterns they were classified as the more advanced. Hyperplastic alveolar nodules (HANs) were focal florid hyperplasias with >100 alveoli in cross section of lobular architecture.

Species comparisons of DNA and protein sequences

Comparisons of human and murine *NOP16* DNA and protein were carried out using FASTA version 35.04 Sept. 22, 2009 (Pearson and Lipman 1988; Hubbard et al. 2009). The consensus sequence for human is (CCDS 43403.1) and for mouse is (CCDS 26531.1). Protein alignments were made using FASTAv35.04 ggsearch (http://fasta.bioch.virginia.edu/fasta_www2/fasta_down.shtml).

Statistics

Tumor incidence was determined by dividing the number of mice with tumors by the total number of WAP-c-Myc and NRL-TGFα mice, respectively. Differences between mouse models were determined using Fisher's Exact Tests. Differences in gene expression between groups were tested using two-tailed ANOVA of log-transformed data. Pearson correlation coefficients were utilized on log-transformed data to describe linear relationships between genes. Significance was set at $P \leq 0.05$.

Results

Mammary histology of nontransgenic FVB/N mice

Twenty-four virgin wild type mice of 2.5–12 months were evaluated and compared to transgenic mice (Table 1; Fig. 1). Two of three mice <4 months of age were classified as stage D and the third was AB. Nine mice 4–6 months were classified as 4 D, 4 AB and 1 L1 (Fig. 1a, b). Twelve mice aged 6.5–12 months were in the following stages: 6 D, 2 AB and 4 L1. Mammary glands contained less than 3% parenchyma and 97% adipocytes on cross sections. In no instance were luminal alveolar cells vacuolated, i.e. hypersecretory, and alveoli and ducts were not distended, although in L1 stage small amounts of dense secretions, at times laminated and presumably calcium, were often seen. Ducts were generally filled with pale secretions but were not dilated, >160 μm diameter, and averaged 125 μm. Cells of the ducts, alveolar buds and alveoli were uniform and without chromatin

clumping, margination or hyperchromasia (Fig. 1c). Nuclei averaged 6.5 μ with the largest <8 μ. Nucleoli were small, uniform, rarely multiple, and <2 μ size. A refractive iron containing pigment was seen occasionally in the cells of alveolar buds and lobules, (Miyawaki 1965) which may vary with the estrous cycle, as pigment was not identified in D stage. Dysplasias, hyperplasias, squamous lesions or tumors were not observed.

Mammary pathology in NRL-TGFα mice

All NRL-TGFα mice between 12–16 weeks of age were similar to controls. Of mice between >16–26 weeks of age, 6/14 mice had alveolar hyperplasia (L2–L3 stage; Fig. 1a) which was accompanied by dilated ducts (11/14; Fig. 1d–f), dilated lobular units (8/14) and abnormal dense and calcified secretions Fig. 1e). Multifocal lesions sometimes displayed more than one architectural pattern, e.g., multiple papillomas (MP) and multiple papillomas with DCIS (MP-DCIS). Histological evaluations were carried out in 26 mice with tumors (Table 2). Tumors were found as early as 26 weeks and were predominantly hypersecretory papillary cystic tumors and occasionally solid adenocarcinomas. Three animals had single solid tumors of alveolar character, two of which were associated with an adjacent MP-DCIS. Solid tumors were Grade 2, one of which was an adenosquamous carcinoma. Hypersecretory vacuoles were present in alveolar cells from glandular regions without tumors and in cells of the cystic tumors (Fig. 1f, i). Eight animals had HANs, often associated with squamous metaplasia, and which always were associated with a marked degree of lobular hyperplasia (L3; Fig. 1d). Cystic and solid tumors were Esr1+/Pgr− as reported previously[12] and did not invade locally or metastasize (Table 2).

Mammary pathology in WAP-c-Myc mice

All c-Myc mice with tumors in this study were >6.5 months and had developed an anaplastic carcinoma of similar type. Animals studied at a younger age demonstrated a uniform precancerous process. Hyperplasia of lobular elements greater than controls was present in 3/4 animals by 2.5 months of age and this was accompanied by slight cellular anaplasia. High-grade anaplasia was widespread in all animals studied at 4 months (Fig. 1j). At this time acinar nuclei were enlarged, hyperchromatic and clumped and exhibited margination and clearing (Fig. 1k–l). Nucleoli were dramatically enlarged and often multiple. Mitotic and apoptotic activity was increased and cells became multilayered filling some alveoli (Fig. 1k–l). Degree of hyperplasia and anaplasia paralleled each other. The dysplastic-hyperplastic features were more prominent in alveoli than in terminal ducts. Hyperplasias occasionally expanded to HANs and in two animals contained portions that transitioned to carcinoma. Myoepithelial cells were present around dysplastic alveoli and in HANs (Fig. 1l) but were not present when dysplasias transformed into malignancy (Fig. 1o). Hyperplasias were ESR1+/PGR− (Fig. 2).

Tumors were present in 6/6 mice ≥6.5 months (Table 1). Tumors were composed of cells similar in appearance to the dysplastic cells in adjacent nontumorous mammary gland but cells were larger, more mitotically active, contained more extensive chromatin abnormalities and retained multiple giant nucleoli (Fig. 1o). Adhering to criteria in common usage for human breast cancers (Elston and Ellis 1991) these would be classified as Grade III tumors. An acinar pattern predominated in smaller tumors but with increased proliferation tumors

become cribiform, trabecular and solid. Despite variable architectural features, cytologic features of high-grade malignancy were uniformly present and 5/6 tumors were ESR1+/PGR − while the remaining case was ESR1−/PGR− (Fig. 2e, h, respectively). Necrosis was evident in most cases as was local and distant metastasis (Table 2).

Protein analysis of mammary glands from WAP-c-Myc and NRL-TGFα mice

Protein analysis of NOP16 in murine cells or tissues has not been carried out previously. Based on DNA and protein sequence analyses of NOP16 which show that mouse and human genes share 84.4% identity and 84.4% similarity while encoded proteins are 91% identical with 98.9% similarity, we surmised that commercial antibodies directed against human proteins would identify protein in mouse tissue. (Sequence comparisons are depicted in Supplemental Materials Online Resource 1). We tested antibodies directed against NOP16 protein, a mouse polyclonal antibody (#88449 from Abcam) and a rabbit polyclonal antibody (H00051491-D01 from Abnova). (Supplemental Materials Online Resource 2). Both primary antibodies identified the same size protein of the expected NOP16 molecular weight, however the anti-mouse HRP conjugated secondary antibody produced a non-specific secondary band. In addition, rabbit polyclonal antibody produced stronger NOP16 signal than the mouse monoclonal antibody. For immunohistochemistry, the mouse monoclonal antibody, but not the rabbit polyclonal antibody resulted in a detectable signal. The mouse monoclonal NOP16 antibody was detectable using a mouse on mouse HRP detection system. We therefore utilized the rabbit polyclonal antibody for western analysis of tumor levels of NOP16 and the mouse monoclonal antibody for immunolocalization of NOP16 protein in tissues sections. Protein extracts from tumors isolated from WAP-c-Myc and NRL-TGFα mice are depicted in Fig. 3a. Protein extracts from tumors isolated from WAP-c-Myc mice contained on average 2.5 fold higher levels of NOP16 than measured in tumors from NRL-TGFα mice ($P = 0.0005$; Fig. 3b).

We also were interested in identifying the cell types and intracellular location of NOP16 protein in tumor-free and tumor containing mammary glands from mice. Using immunohistochemistry, we identified NOP16 protein in the nuclei and cytoplasm of luminal cells of normal ducts and alveoli (Fig. 4a) as well as in hyperplasias (Fig. 4b), with the most prominent staining in the nuclei. NOP16 antibody staining could not be detected in myoepithelial cells. Similar to earlier reports (Butt et al. 2008), intense nucleolar NOP16 staining was seen in sections of normal luminal epithelial cells (Fig. 4b). In addition, NOP16 staining was stronger in the nucleus than in the cytoplasm of cells residing in cystic tumors obtained from TGFα mice and most epithelial cells stained positively. In sections taken from the same tumor, more cells were positively stained with NOP16 antibody than with ESR1 antibody (Fig. 4d). In tumors from WAP-c-Myc mice, however, NOP16 staining was weak or absent in the nucleus of tumor cells but prevalent in the cytoplasm. It was unlikely that cytoplasmic staining is attributed to background staining as western blot analysis pointed to a 2-fold increase on average of NOP16 in tumors from WAP-c-Myc mice compared to levels in tumors from NRL-TGFα mice. NOP16 staining distribution was uniform within and between cells of the tumor, but not in the stromal compartment as depicted in the representative photo in Fig. 3e. In contrast, ESR1 staining in tumor cells of tumors from WAP-c-Myc mice, as in tumors from NRL-TGFα mice, had a heterogeneous

pattern of nuclear staining intensity but MYC tumors (Figs. 4f, 2e) and hyperplasias (2d) displayed a uniform cytoplasmic staining intensity that was not present in cells of normal ductal and lobular structures (2c).

Gene co-expression analysis of mammary glands from WAPc-Myc and NRL-TGFα mice

Much of the downstream response to estrogen signaling is due to the upregulation of MYC signaling. In addition, indirect measurement of estrogen signaling is through the evaluation of (ESR1) and progesterone receptor (PGR) protein status of breast cancers and the presence of these biomarkers dictate treatment options, specifically the presence of receptors is required for utility of selective estrogen receptor modulators. We previously described the pattern of expression of *Esr1* and *Pgr* transcripts and protein in mammary glands and tumors from NRL-TGFα mice (Rose-Hellekant et al. 2007). Hyperplasias and tumors are ESR1/PGR-although luminal cells from normal appearing ducts and lobules display ESR1 and PGR protein in proportions similar to nontransgenic mice. Transcript levels reflected protein levels, as *Esr1* and *Pgr* mRNA amounts were greatly reduced in hyperplasias and tumors compared to nontumor containing mammary glands. However, we have not previously characterized the pattern of expression of these transcripts in mammary glands from WAP-c-Myc mice. Tumors from WAP-c-Myc mice are ESR1+/PGR− and *Esr1* and *Pgr* transcript levels in tumors were significantly lower than nontumor containing glands (Fig. 2a).

We hypothesized that tumor environments with relatively high *Myc* levels would have different coexpression patterns of Nop16 than tumor environments with relatively low *Myc* levels. We first measured *Nop16* and *Myc* levels in tumors from WAP-c-Myc and NRL-TGFα mice and verified that indeed tumors from WAP-c-Myc mice expressed significantly higher levels of both transcripts, 10-fold higher *Nop16* and 32-fold higher *Myc* on average, than tumors from NRL-TGFα mice (Fig. 5a, b). Because previous studies have shown that *Myc* and *Esr1* are transcriptionally regulated by estrogen, we then correlated *Myc* and *Esr1* mRNA levels in tumors from both WAP-c-Myc and NRL-TGFα mice. *Myc* and *Esr1* transcript levels in tumors from both transgenic mouse lines were highly correlated with correlation coefficients that were similar (Fig. 5c, d), suggesting that MYC levels do not alter Esr1 transcriptional regulation. We also measured *Nop16* transcript levels and found that tumor containing glands from WAP-c-Myc mice had approximately 50-fold higher levels of *Nop16* mRNA than nontumor containing glands from the same mouse line while *Nop16* transcript levels in tumors from NRL-TGFα mice were significantly lower by approximately 10-fold (Fig. 5a). These data confirm that tumors with higher *Myc* levels also have higher *Nop16* levels.

In previous reports *Nop16* transcript levels correlate with *Myc* levels in breast cancer cell lines and furthermore, *Nop16* transcription was induced by MYC directly, and by estrogen indirectly through *Myc* upregulation (Butt et al. 2008). However, coherence of *Myc* and *Nop16* coexpression was reduced in clinical breast tumors. We therefore evaluated whether *Nop16* expression levels correlated with *Myc* levels in murine mammary tumors. We found that *Nop16* transcript levels positively correlated to *Myc* levels in tumors from NRL-TGFα mice (Fig. 5e; r = 0.9183 $P \leq 0.0011$) but not in tumors from WAP-c-Myc mice (Fig. 5f; r =

0.3477; $P = 0.128$). These data support the hypothesis that *Nop16* transcript levels are regulated differently in tumor environments with relatively high versus low *Myc* levels.

Discussion

We were motivated to carry out these evaluations in mice because of inconsistent observations of *NOP16* expression patterns previously reported in human breast cancer cell lines and clinical breast cancers. We reasoned that *NOP16* expression dynamics in human breast cancers could be accurately modeled in murine mammary cancers. High DNA and protein sequence identities and similarities for human and mouse NOP16 (Online Resource 1), as well as comparable biological activities of MYC and ESR1 in breast/mammary carcinogenesis in these two species support this supposition. Although part of the nucleolar proteome, little is known about NOP16 function (Schlosser et al. 2003). *NOP16* was identified as a MYC and estrogen target gene in breast cancer cell lines for which higher levels were associated with cell lines with an aggressive phenotype (Lin et al. 2004; McNeil et al. 2006; Dai and Lu 2008; Musgrove et al. 2008). Correlations between *NOP16* and *MYC* mRNA levels also was shown in human breast tumors, although significantly less robust than that found in cell lines. Importantly, patients with the highest levels of tumor *NOP16* had poorer survival outcomes than those with tumors expressing the lowest levels of *NOP16* (Butt et al. 2008). However, NOP16 levels were similar in clinical breast cancers classified as ESR1+ or ESR1−: an inconsistent finding compared to observations in human breast cancer cells lines for which *NOP16* transcription was induced by estrogen. These inconsistencies point to a complex picture of *NOP16* regulation by MYC and estrogen.

We first determined whether high levels of mouse tumor *Nop16* mRNA were associated with aggressive tumor phenotype as determined by histopathology. We evaluated murine mammary glands during early and late stages of tumorigenesis using a standard system that emulates human pathological evaluations (Cardiff et al. 2000). Tumors in WAP-c-Myc mice were clearly more aggressive than in NRL-TGFα mice, although we found pronounced cellular atypia that progressed with the development of hyperplasias, dysplasias and tumors in both mouse models (Fig. 1). Multiple nucleoli as well as a high level of proliferative activity were often found in epithelial cells making up the lesions from both mouse lines (Fig. 1l, o), however, these features were clearly more aggressive in WAP-c-Myc mice. In addition, tumors in WAP-c-Myc mice developed faster than tumors in NRL-TGFα mice. Tumors from WAP-c-Myc mice were classified as high grade adenocarcinomas and had a high incidence of local invasion and metastasis while NRL-TGFα mice typically developed low to medium grade cystic hypersecretory in situ carcinomas that did not invade locally or metastasize (Table 2). Tumors from WAP-c-Myc mice expressed relatively low levels of *Esr1* and *Pgr* mRNA levels compared to nontumor containing glands. PGR protein levels were below detection for all tumors (Fig. 2h) but ESR1 protein was readily detectable in all tumors with one exception, suggesting a high mRNA turnover and stable protein (Fig. 2e). Using quantitative RT–PCR mentods, we found markedly higher levels of *Nop16* mRNA in murine tumors with aggressive phenotype concurring with previous reports in human breast cancers.

We next evaluated NOP16 protein levels in murine mammary tissue. Using western blot analysis of tumor lysates we confirmed that NOP16 protein levels were significantly higher in tumors from WAP-c-Myc mice than in NRL-TGFα mice. In addition, we identified the location of NOP16 protein to be in normal ducts and alveoli, hyperplasias and tumors. Nuclear and nucleolar staining was evident in luminal epithelial cells of mammary ducts, alveoli and hyperplasias as well as in tumor epithelial and stromal cells from NRL-TGFα mice. Tumor cells from WAP-c-Myc mice, however, displayed faint or undetectable nuclear staining, but cytoplasmic staining was detectable and uniformly distributed throughout most tumor cells. Tumors in WAP-c-Myc mice had high levels of *Nop16* mRNA indicating high rates of transcription. The lack of nuclear NOP16 protein in high-grade tumors from WAP-c-Myc mice appears to conflict with data by others who identified NOP16 in nucleoli of cells in culture and presumed involvement in ribosomal biogenesis.

One possible explanation for cytoplasmic location of NOP16 is that not all ribosomal associated proteins have a function in ribosomal biogenesis; it has been reported that only approximately one-third of nucleolar proteins are involved in transcription and processing of ribosomal RNA and ribosomal proteins. The other ribosomal residing proteins can function in cell cycle regulation, DNA damage repair, pre-mRNA processing, RNA editing, telomere metabolism, rRNA processing, and regulation of protein stability (reviewed by Lam and Trinkle-Mulcahy 2005). In addition, many proteins that are associated with ribosomal biogenesis move between nucleolar, nuclear and cytoplasmic locations during maturation. With these considerations in mind, the fact that we identified a shift in the location of *NOP16* from predominantly the nucleus to the cytoplasm may be due to either the upregulation of transcription, translation and overall ribosomal biogenesis or to the increased production of other cellular proteins not involved with ribosomal biogenesis. In either case, the levels of NOP16 would be expected to be more robust in high grade cancers relative to levels in low grade cancers or normal cells. In addition, the increased and aberrant proteasomal activities are common features in cancers (Chen and Dou 2010) and may explain the staining pattern disparities between Myc tumors versus normal epithelial structures and the relatively low grade TGFα tumors.

Tumor NOP16 levels were strong predictors of adverse outcome in breast cancer patients (Butt et al. 2008). This same group reported co-expression of *NOP16* and *MYC* mRNA in human breast cancers was low ($r^2 = 0.19$; Butt et al. 2008) compared to breast cancer cell lines ($r^2 = 0.60$). We therefore reasoned that *Nop16* transcription or transcript stability may be different in high versus low MYC tumor *milieu. Myc* mRNA levels were on average 32 fold higher in tumors from WAP-c-Myc mice than in tumors from NRL-TGFα mice, while *Nop16* levels were on average 50 fold higher (Fig. 5). We demonstrated that levels of *Esr1* and *Myc* transcripts in tumors from both WAP-c-Myc and NRL-TGFα mice are strongly correlated (Fig. 5c, d), but correlation of expression levels between *Nop16* and *Myc* existed only in tumors from NRL-TGFα mice (Fig. 5e). There was no correlation between these transcripts in tumors from WAP-c-Myc mice (Fig. 5f), indicating that regulation of *Nop16* transcription and/or mRNA stability may be influenced by the tumor environment.

Our results from murine mammary tumors were similar to those generated in human breast cancers in that they point to a transcriptional relationship between estrogen, *Myc* and *Nop16*

in some biological contexts but not all. One marked difference between tumor types is the relative level of *Myc* expression. Since MYC is a key determinant of aggressive cancer phentoype and has been shown previously to directly regulate *NOP16* transcription, it is possible that transcriptional regulation is different in tumor environments with low versus high MYC levels. The previous study for which *NOP16* and *MYC* mRNA levels were evaluated in clinical breast cancers did not stratify tumors based on *MYC* levels, so direct comparisons of the congruency between these transcripts in tumors from mice and humans cannot be drawn (Butt et al. 2008). However, highly aggressive tumors often have high levels of *MYC* due to gene overexpression or amplification. In addition, although endocrine therapy is only effective in patients with ESR1+ cancers, endocrine resistance is frequent. Tumors with high MYC expression has been suggested to be an important factor in endocrine resistance of ESR1+ breast cancer (Liao and Dickson 2000; McNeil et al. 2006). In addition, approximately 10–15% of genes in the human genome are estimated to be modulated by MYC providing a large number (Chung and Levens 2005). Taken together, the influence of MYC on transcription is significant and likely modifies the activities of other cancer related genes including ESR1 and NOP16.

Differential coexpression analysis (Fang et al. 2010) is used when a coexpressed cohort of genes has a high level of coherence in one subset of samples but lower coherence in another. The application of differential coexpression analysis to breast cancers with high versus low MYC expression may reveal unique transcriptional rules that occur in differing cancer contexts. Stratifying clinical breast cancers by MYC may improve our ability to utilize cancer biomarkers more effectively.

In summary, we confirmed that NOP16 levels are similarly elevated in high grade tumors compared to low grade tumors in mice as has been demonstrated previously in human breast cancer cases. In addition, we demonstrated that *Nop16* co-expression pattern with *Myc*, but not *Esr1*, differs in tumor environments that are molecularly and histopathologically dissimilar. Overexpression or amplification of the MYC oncogene, a key regulator of transcription in humans and mice may be a determining event that influences gene coexpression patterns in breast cancers. Identifying the consequences of differential gene coexpression in breast cancers stratified by MYC is therefore an important first step. These findings support the utility of transgenic mouse models to further study regulation and biological function of NOP16 as well as its relevance as a breast cancer biomarker.

Supplementary Material

Refer to Web version on PubMed Central for supplementary material.

Acknowledgments

The authors greatly appreciate the assistance of Barbara Elmquist and Emily Heid for excellent preparation of tissues for histologic and immunohistochemical review and Drs. Jon Holy and Lois Heller for critical review of this manuscript. This work was supported by NIH grant K01-RR00145, the University of Minnesota Medical Foundation the Academic Health Center to TRH, the University of Minnesota Undergraduate Research Opportunities Program to ES and by St. Luke's Hospital-Duluth.

References

Ahmad Y, Boisvert FM, Gregor P, Cobley A, Lamond AI. NOPdb: nucleolar proteome database–2008 update. Nucleic Acids Res. 2009; 37:D181–D184. [PubMed: 18984612]

Butt AJ, Sergio CM, Inman CK, et al. The estrogen and c-Myc target gene HSPC111 is over-expressed in breast cancer and associated with poor patient outcome. Breast Cancer Res. 2008; 10:R28–R38. [PubMed: 18373870]

Cardiff RD, Anver MR, Gusterson BA, et al. The mammary pathology of genetically engineered mice: the consensus report and recommendations from the Annapolis meeting. Oncogene. 2000; 19:968–988. [PubMed: 10713680]

Chen D, Dou QP. The ubiquitin-proteasome system as a prospective molecular target for cancer treatment and prevention. Curr Protein Pept Sci. 2010; 11(6):459–470. [PubMed: 20491623]

Chung HJ, Levens D. c-myc expression: keep the noise down! Mol Cells. 2005; 20:157–166. [PubMed: 16267388]

Dai MS, Lu H. Crosstalk between c-Myc and ribosome in ribosomal biogenesis and cancer. J Cell Biochem. 2008; 105:670–677. [PubMed: 18773413]

Elston CW, Ellis IO. Pathological prognostic factors in breast cancer. I. The value of histological grade in breast cancer: experience from a large study with long-term follow-up. Histopathology. 1991; 19:403–410. [PubMed: 1757079]

Fang G, Kuang R, Pandey G, Steinbach M, Myers CL, Kumar V. Subspace differential coexpression analysis: problem definition and a general approach. Pac Symp Biocomput. 2010:145–156. [PubMed: 19908367]

Geyer FC, Lopez-Garcia MA, Lambros MB, Reis-Filho JS. Genetic characterisation of breast cancer and implications for clinical management. J Cell Mol Med. 2009

Hubbard TJ, Aken BL, Ayling S, et al. Ensembl 2009. Nucleic Acids Res. 2009; 37:D690–D697. [PubMed: 19033362]

Lam YW, Trinkle-Mulcahy L. Lamond AI: the nucleolus. J Cell Sci. 2005; 118:1335–1337. [PubMed: 15788650]

Leung AK, Trinkle-Mulcahy L, Lam YW, Andersen JS, Mann M, Lamond AI. NOPdb: nucleolar proteome database. Nucleic Acids Res. 2006; 34:D218–D220. [PubMed: 16381850]

Liao DJ, Dickson RB. c-Myc in breast cancer. Endocr Relat Cancer. 2000; 7:143–164. [PubMed: 11021963]

Lin CY, Strom A, Vega VB, et al. Discovery of estrogen receptor alpha target genes and response elements in breast tumor cells. Genome Biol. 2004; 5:R66. [PubMed: 15345050]

Ma CX, Sanchez CG, Ellis MJ. Predicting endocrine therapy responsiveness in breast cancer. Oncology (Williston Park). 2009; 23:133–142. [PubMed: 19323294]

McNeil CM, Sergio CM, Anderson LR, et al. c-Myc overexpression and endocrine resistance in breast cancer. J Steroid Biochem Mol Biol. 2006; 102:147–155. [PubMed: 17052904]

Miyawaki H. Histochemistry and electron microscopy of iron-containing granules, lysosomes, and lipofuscin in mouse mammary glands. J Natl Cancer Inst. 1965; 34:601–623. [PubMed: 14313820]

Morin RD, O'Connor MD, Griffith M, et al. Application of massively parallel sequencing to microRNA profiling and discovery in human embryonic stem cells. Genome Res. 2008; 18:610–621. [PubMed: 18285502]

Musgrove EA, Sergio CM, Loi S, et al. Identification of functional networks of estrogen- and c-Myc-responsive genes and their relationship to response to tamoxifen therapy in breast cancer. PLoS One. 2008; 3:e2987. [PubMed: 18714337]

Nygaard S, Jacobsen A, Lindow M, et al. Identification and analysis of miRNAs in human breast cancer and teratoma samples using deep sequencing. BMC Med Genomics. 2009; 2:35. [PubMed: 19508715]

Pearson WR, Lipman DJ. Improved tools for biological sequence comparison. Proc Natl Acad Sci USA. 1988; 85:2444–2448. [PubMed: 3162770]

Perou CM, Sorlie T, Eisen MB, et al. Molecular portraits of human breast tumours. Nature. 2000; 406:747–752. [PubMed: 10963602]

Rose-Hellekant TA, Sandgren EP. Transforming growth factor alpha- and c-myc-induced mammary carcinogenesis in transgenic mice. Oncogene. 2000; 19:1092–1096. [PubMed: 10713695]

Rose-Hellekant TA, Schroeder MD, Brockman JL, et al. Estrogen receptor-positive mammary tumorigenesis in TGFalpha transgenic mice progresses with progesterone receptor loss. Oncogene. 2007; 26:5238–5246. [PubMed: 17334393]

Sandgren EP, Schroeder JA, Qui TH, Palmiter RD, Brinster RL, Lee DC. Inhibition of mammary gland involution is associated with transforming growth factor alpha but not c-myc-induced tumorigenesis in transgenic mice. Cancer Res. 1995; 55:3915–3927. [PubMed: 7641211]

Schlosser I, Holzel M, Murnseer M, Burtscher H, Weidle UH, Eick D. A role for c-Myc in the regulation of ribosomal RNA processing. Nucleic Acids Res. 2003; 31:6148–6156. [PubMed: 14576301]

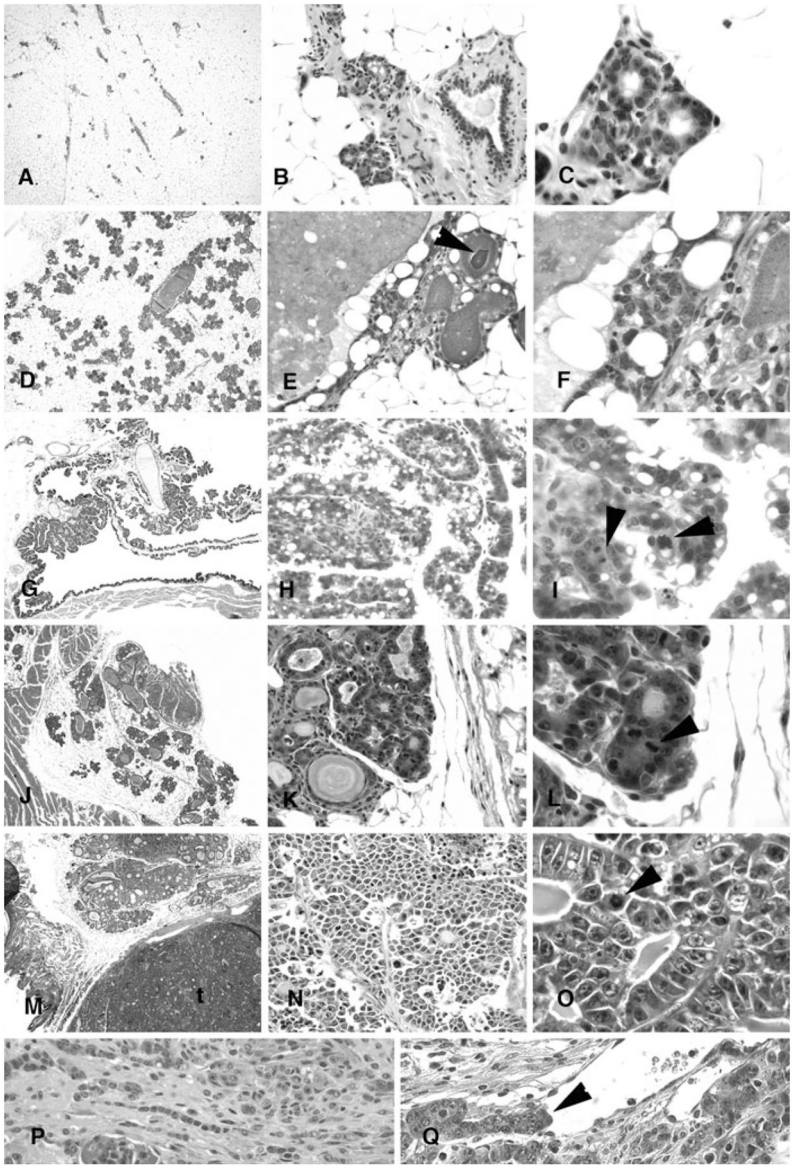

Fig. 1.

Mammary gland morphology in virgin nontransgenic (**a–c**), NRL-TGF*α* (**d–i**) and WAP-c-Myc (**j–q**) mice in the FVB/N strain. **a** Gland from a 6-month old mouse in AB stage. Note absence of alveolar hyperplasia. 40x. **b** Mammary duct in L1 stage with alveolar budding from a 4-month old mouse. 400x. **c** The same mammary gland as **b**. Note small uniform cell size, bland uniform chromatin and absence of enlarged nucleoli. 1000x. Mammary gland histology of NRL-TGF*α* virgin mice at 6 months (**d–f**) and 8.5 months and (**g–i**) **d** Cystic dilation of ducts and widespread prominent alveolar hyperplasia (L2 stage). 40x. **e** Epithelial hyperplasia produces multiple layers of cells lining the cysts. Dense staining secretions are evident in ducts and alveoli (*arrowhead*). 400x. **f** Multiple layers of epithelial cells line a cyst. Epithelia contain cytoplasmic secretory vacuoles. Note relatively bland nuclear features. 1000x. **g** Dilated cyst lined with multiple papilloma. 40x. **h** Hypersecretory cells lining papillary cyst. **i** Papillary structure with nuclear variability and high levels of mitoses

(arrowheads). **j** Gland from a 4.5 month WAP-c-Myc mouse. At this age all show hyperplasias of lobules and ductal dilatation. L2 stage. 40x. **k** Same mammary gland as J displaying hyperplastic lobules of irregular shape. 400x. **l** Same mammary gland as J and K displaying alveolar cells that are enlarged, hyperchromatic with clearing and margination of chromatin, nucleoli which are markedly enlarged, frequent mitoses (*arrowhead*) and foci of alveolar cells which pile up into several layers. 1000x. **m** Gland from a 6.5 month old WAP-c-myc mouse displaying hyperplasia of marked degree (L3 stage) and adjacent tumor (t). 40x. **n** Same gland as M, displaying an anaplastic adenocarcinoma with solid and glandular areas. 400x. **o**. Same gland as M and N. Note accentuated but similar features of tumor cells to dysplasia seen in L. Cells are enlarged, hyperchromatic, with clumped chromatin and nuclear clearing. Nucleoli are markedly enlarged and mitosis frequent (arrowhead). 1000x. **p** Stromal invasion (400x) and **q** vascular invasion (400x) seen in a 6.5 month old WAP-c-Myc mouse

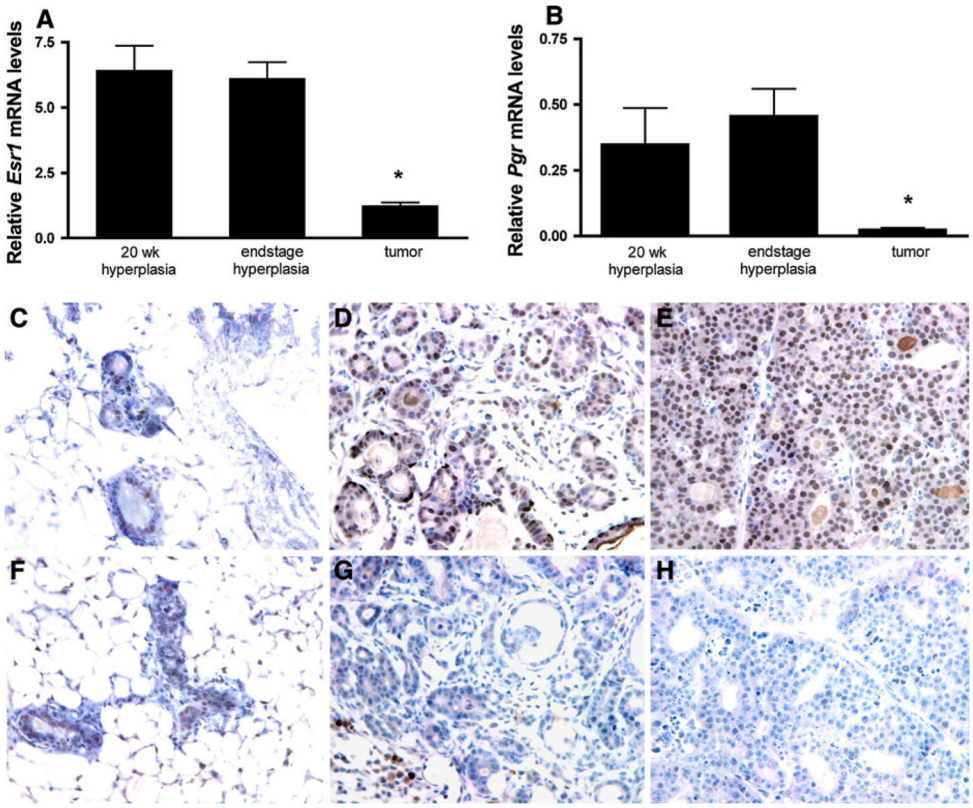

Fig. 2.

Relative levels of *Esr1* and *Pgr* mRNA and protein in mammary glands from mice. (**a**) *Esr1* and *Pgr* mRNA transcripts in WAP-c-Myc mice during different stages of tumorigenesis. *Esr1* and *Pgr1* levels were reduced in tumors compared with hyperplastic glands. Transcript levels were normalized to the housekeeping gene *Pum1*. Endstage hyperplasias were collected from contralateral glands at the same time as tumors. (**b**) ESR1 (**c–e**) and PGR (**f–h**) protein is present in normal ducts and alveoli (**c, f**) of wild type FVB/N mice and in glandular hyperplasias of WAP-c-Myc mice (**d, g**). Myc tumors are ESR1+/PGR− (**e, h**) Brown stain indicates protein immunolocaliztion. Photos are 400x magnification

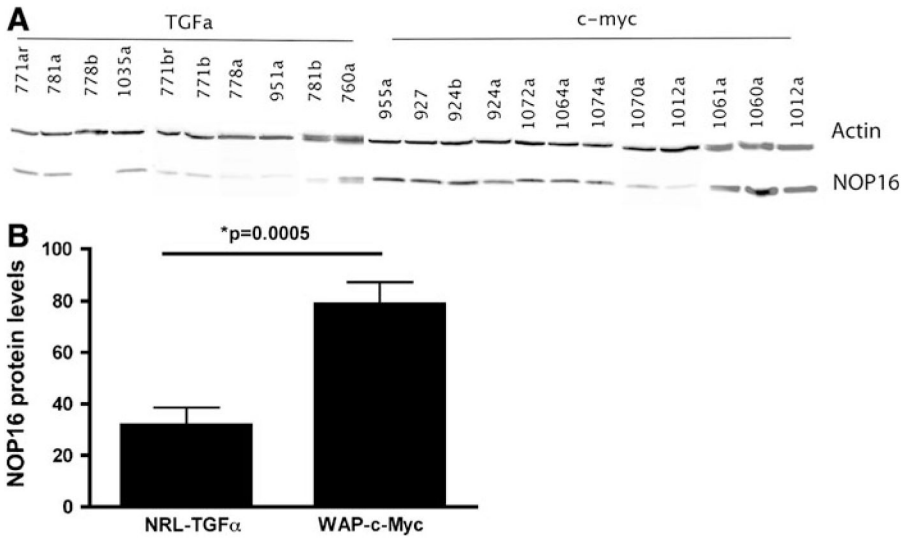

Fig. 3.

a Western blot of protein lysates isolated from tumors of NRL-TGFα (n=12) and WAP-c-Myc (n-10) mice. **b** Protein extracts from tumors isolated from WAP-c-Myc mice contained on average 2.5 fold higher levels of NOP16 than measured in tumors from NRL-TGFα mice (P = 0.0005). NOP16 protein levels were normalized to actin levels

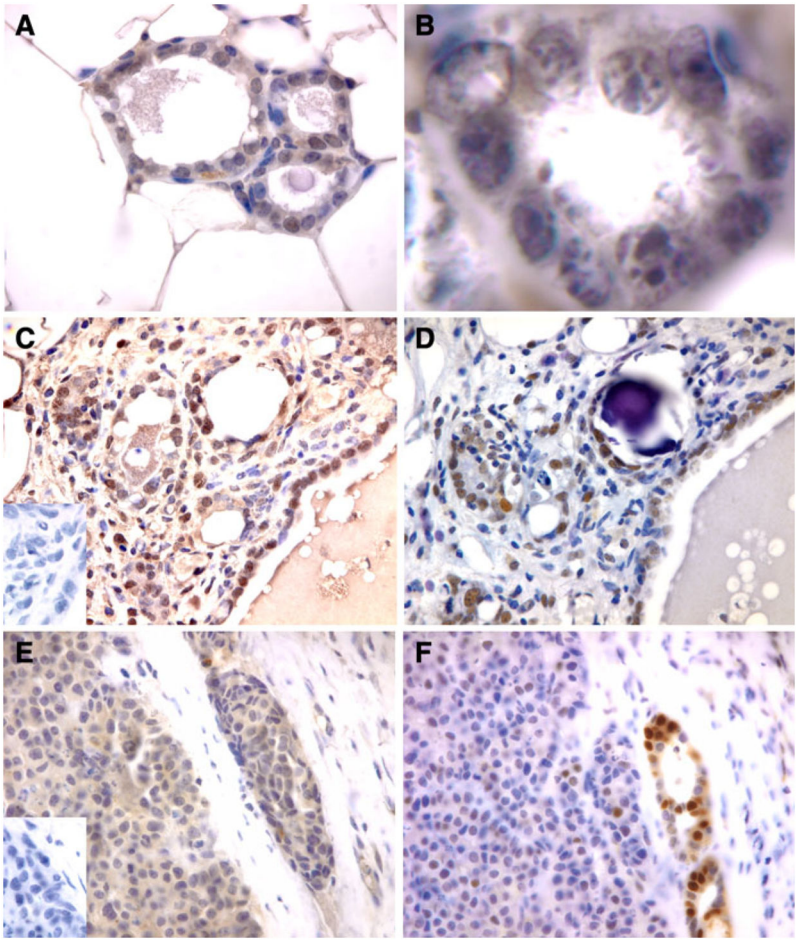

Fig. 4.

NOP16 protein staining patterns in murine mammary glands. **a** NOP16 antibody staining was evident predominantly in the nucleus but also in the cytoplasm of luminal but not myoepithelial cells. 400x magnification. **b** Intense brown staining indicating higher levels of NOP16 within the nucleoli of luminal epithelial cells. 1000x microscopic magnification with 3.9 fold computer magnification. **c–f** Comparison of NOP16 (**c**, **e**; 400x magnification) and ESR1 (**d**, **f**; 400x magnification) antibody staining in epithelial and stromal cells in neighboring sections of tumors from NRL-TGFα mice (**c**, **d**) and WAP-c-Myc mice (**e**, **f**). Note predominantly nuclear staining of NOP16 in tumors from NRL-TGFα mice and cytoplasmic staining in tumors from WAP-c-Myc mice. Control sections without primary NOP16 antibody but otherwise treated similarly are provided as inserts in **c** and **e**

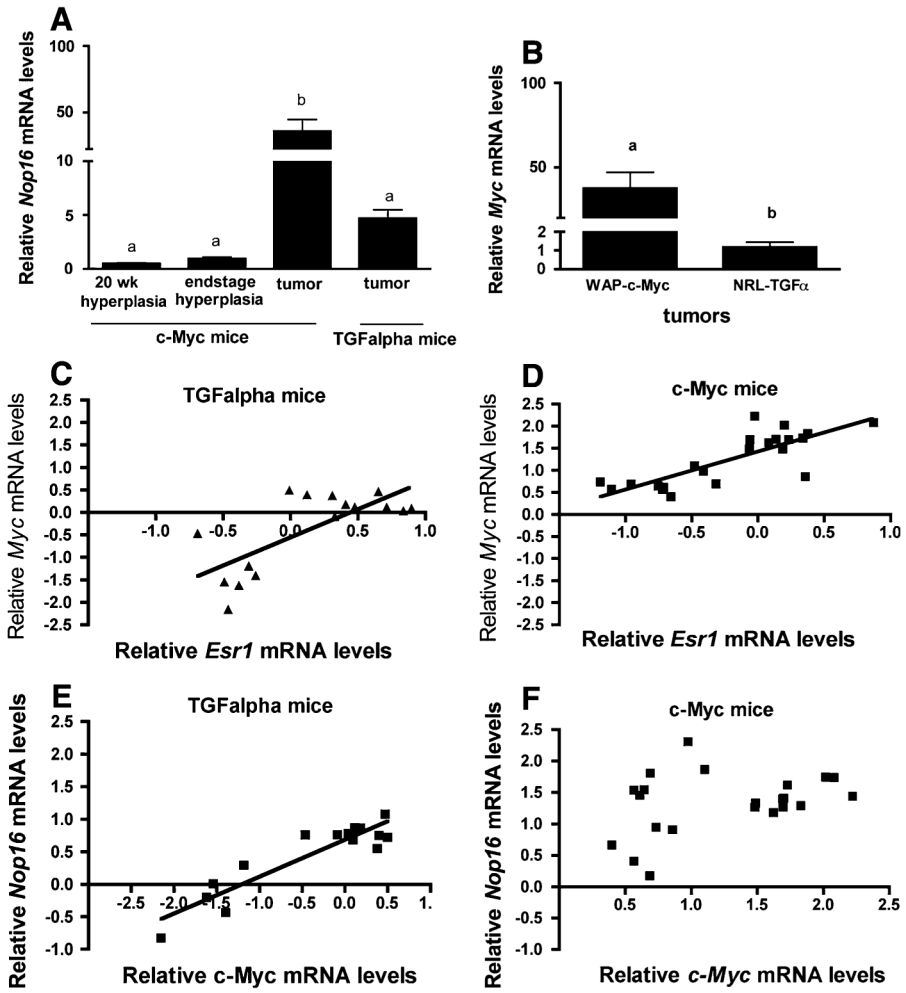

Fig. 5.

Nop16 mRNA levels in mammary glands from WAP-c-Myc and NRL-TGFα mice and co-expression with *Myc* and *Esr1* in tumors. **a** *Nop16* mRNA levels were normalized to levels of the housekeeping gene, *Pum1*, in mammary glands from WAP-c-Myc mice during different stages of tumorigenesis and tumors from NRL-TGFα mice. *Nop16* levels were greatly enhanced in tumors compared to glands with hyperplasias in c-Myc mice. In addition tumors from c-Myc mice had significantly more *Nop16* than in tumors from TGFα mice. **b** *Myc* levels were approximately 32-fold higher in tumors from WAP-c-Myc versus NRL-TGFα mice. *Different letters* above *bars* in graph represent groups which are statistically different at $P \leq 0.05$. **c, d** *Nop16* mRNA levels are correlated to *Esr1* mRNA levels in tumors from both NRL-TGFα mice (Pearson r = 0.7335; $P < 0.0012$) and WAP-c-Myc mice (r = 0.8095; $P < 0.0001$). **e, f** *Nop16* mRNA levels correlate with *Myc* mRNA levels in tumors from NRL-TGFα (Pearson r = 0.9183; $P = 0.0001$) but not WAP-c-Myc mice (Pearson r = 0.2927; $P = 0.183$). Tumors from 22 WAP-c-Myc mice and 16 NRL-TGFα mice were analyzed

Table 1

Mammary tumor incidence by age group

	Tumor incidence in FVB/N mouse strains (mice with tumors/mice evaluated)		
Age (weeks)	**Nontransgenic (total n = 24)**	**WAP-c-Myc (total n = 17)**	**NRL-TGFα (total n = 42)**
<16	0/3	0/4	0/2
16–26	0/10	0/7	3/14
>28	0/11	6/6	24/26

Table 2

Physical characteristics of mammary tumors from transgenic mice

	Incidence per tumor	
Characteristic	**WAP-c-Myc**	**NRL-TGF*α*[a]**
Histotype	Solid adenocarcinoma 6/6	Hypersecretory papillary cystic tumors 26/29 Solid adenocarcinoma 3/29
Grade	III: 6/6*	I: 6/29 II: 23/29
Necrosis	5/6*	0/29
Stromal invasion	4/6*	0/29
Vascular invasion	3/6*	0/29
Lymph node metastasis	0/6	0/29
Lung metastasis	11/14*	None grossly evident
Liver metastasis	2/10*	None grossly evident

[a] 29 tumors were evaluated in 26 NRL-TGF*α* mice

* Statistically differences between WAP-c-Myc and NRL-TGF*α* mice.

Significance levels at $P < 0.05$ Fisher's Exact Test